

NORSAR Scientific Report No. 1-93/94

# **Semiannual Technical Summary**

**1 April — 30 September 1993**

Kjeller, November 1993

**APPROVED FOR PUBLIC RELEASE, DISTRIBUTION UNLIMITED**

## 7 Summary of Technical Reports / Papers Published

### 7.1 Continuous threshold monitoring of the Lop Nor, China, test site

#### *Introduction*

The continuous threshold monitoring technique (Ringdal and Kværna, 1989) represents a new approach toward achieving reliable seismic monitoring for the purpose of verifying nuclear test ban treaties.

Traditionally, seismic monitoring has relied upon applying signal detectors to individual stations within a monitoring network, associating detected phases and locating possible events in the region of interest. This procedure has been accompanied by assessments of network capabilities for the target region, usually by applying statistical models for the noise level distribution, introducing station corrections for signal attenuation and devising a combinational procedure to determine the detection threshold as a function of the number of phase detections required for reliable location.

The statistical noise models used in these capability assessments are not able to accommodate the effect of interfering signals, such as the coda of large earthquakes, which may cause the estimated thresholds to be quite unrealistic at times. Furthermore, only a statistical capability assessment is achieved, and no indication is given as to particular time intervals when the possibility of undetected clandestine explosions is particularly high.

The continuous threshold monitoring technique alleviates these problems. It makes it possible to ascertain, at any point in time, for a given target region, the maximum magnitude of a possible clandestine explosion at a predefined level of confidence. This makes it possible to focus attention upon those specific time intervals when realistic evasion opportunities exist, while retaining confidence that no treaty violation has occurred at other times.

The continuous threshold monitoring technique has previously been applied experimentally in connection with the Novaya Zemlya test site (Ringdal and Kværna, 1992; Kværna, 1992). This test site is within regional distance of the Fennoscandian arrays, and consequently an excellent monitoring capability ( $m_b \sim 2.5$ ) has been achieved for this site.

#### *Application to the Lop Nor test site*

In order to further demonstrate how continuous threshold monitoring could be performed in a practical operation situation, we have conducted an experiment during which we have applied continuous threshold monitoring to the Chinese test site at Lop Nor for a five-day period. Our data base has been the regional array network NORESS, ARCESS and GERESS. As illustrated in Fig. 7.1.1, these three arrays are all at teleseismic distances from the test site, with excellent P-phase detection capabilities (see Fig. 7.1.2). In particular, the NORESS array has an excellent detection capability for this test site.

The parameters used in the threshold monitoring experiment are given in Table 7.1.1. For each array, we steer "optimum" P beams towards the test site, and calibrate these beams

using actually observed signal attenuation from previous Lop Nor explosions. By focusing in this way on the target region, we can at any point in time measure the "noise magnitude" for a given phase at a given array, and combine these data to obtain a network threshold as explained in detail by Ringdal and Kværna (1989).

### *Results*

Figs. 7.1.3-7.1.7 show the results of the monitoring experiment. Each of these figures covers one data day, starting 1 October 1993. The upper three traces of each figure represent the thresholds (i.e., 90% upper magnitude limits) obtained from the three individual arrays, whereas the bottom trace illustrates the network threshold. Typically, the individual array traces have a number of significant peaks for each 24-hour period, due to interfering events (local or teleseismic). On the network trace, the number and sizes of these peaks are greatly reduced, because an interfering event will usually not provide matching signals at all the stations. From probabilistic considerations, it can in such cases be inferred that the actual network threshold is lower than these individual peaks might indicate.

We will not discuss in detail the individual peaks on the network trace. Here, we will just note that on 2 October (day 275) an aftershock sequence occurred in the S. Sinkiang province. Furthermore, the last day, 5 October 1993, was the day of an actual nuclear explosion ( $m_b = 5.9$ ) at Lop Nor, and this event naturally stands out on the plot. The peak value of the network threshold plot does not represent the actual magnitude of the event, but is slightly lower (see discussion below).

As a general comment to Figs. 7.1.3-7.1.7, we note that such plots are a useful supplement to the Intelligent Monitoring System (IMS) (Bache et al, 1993), and will enable the analyst to obtain an instant assessment of the actual threshold level of the monitoring network. The peaks on the network traces may be quickly correlated with the IMS detection bulletin, in order to decide whether they originate from interfering events or from events in the target region.

### *Discussion*

In a monitoring situation, it will be important to isolate and analyze more extensively those time intervals which offer significant evasion opportunities. Table 7.1.2 gives a statistic of the number of occasions during which the upper magnitude limit exceeded a given level. In theory, if this limit is, e.g., at 4.0, it might be possible that a clandestine  $m_b = 4.0$  explosion had occurred without being detected. There are many options available to investigate such a hypothesis in more detail, although we have not attempted to do so in this study. The most immediate approach would be to analyze high-frequency signals for the time interval being considered.

It is significant that the 3-array network studied in this paper can monitor the Lop Nor test site down to  $m_b$  3.5 or below more than 99% of the time (Fig. 7.1.8). Further improvements would clearly be possible by adding more stations to the monitoring network, especially highly sensitive stations at other azimuths than those covered by the northern

European network. This would in particular contribute to lowering the peaks due to interfering events, whereas any event truly originating in the target region would of course still stand out clearly on the combined network traces.

As a final comment, we will address the apparent contradiction that the magnitude at the time of the nuclear explosion on the threshold trace is slightly lower than the actual event magnitude. In order to explain this, we recall that the network TM calculation assumes that a "hidden" signal is "less than or equal to" the actually observed trace value for each station. While this is a correction assertion for each individual station, it can create a bias if used in a network context, assuming that there is a detectable signal present.

Strictly speaking, this model should only be used during periods with non-detectable signals, or when detections occur from events outside the target area. If there is a detection that could possibly correspond to an event in the target region, "equal" should be used instead of "less than or equal". Hence, the "worst case" (upper 90% limit) magnitude in this case would be the 90 per cent quantile of the distribution for the maximum-likelihood  $m_b$  estimate.

If this philosophy is adopted in calculating the threshold traces, it will result in a slightly increased height of the peaks that are consistent (in azimuth and velocity) with events in the target region. The "background" threshold level will not change, and the peaks that can be confidently assigned to events in other regions will be reduced in the same way as before. The resulting threshold trace computations will be slightly more complex in those cases where peaks at individual stations occur.

The above considerations amplify the importance of using TM *in combination with* a conventional detection/location system. Used in this way, a detectable event will be processed in the conventional way, whereas upper magnitude limits of non-detectable events will be provided by the TM method.

**F. Ringdal**

**T. Kværna**

*References*

- Bache, T.C., S.R. Bratt, H.J. Swanger, G.W. Beall and F.K. Dashiell (1993): Knowledge-based interpretation of seismic data in the Intelligent Monitoring System, *Bull. Seism. Soc. Am.*, 83, 1507-1526.
- Kværna, T. (1992): Continuous seismic threshold monitoring of the northern Novaya Zemlya test site: Long-term operational characteristics; *Report PL-TR-92-2118*, Phillips Laboratory, Hanscom AFB, MA, USA.
- Ringdal, F. and T. Kværna (1989): A multichannel processing approach to real time network detection, phase association and threshold monitoring, *Bull. Seism. Soc. Am.*, 79, 1927-1940.
- Ringdal, F. and T. Kværna (1992): Continuous seismic threshold monitoring, *Geophys. J. Int.*, 111, 505-514.

Station	Phase	Tr. Time	App. Vel.	Azim.	Filter	Config.	STA_len.	Tim. Tol.	Sta_calib.
ARC	P	479.7	13.1	84.8	2-4Hz	A0,C,D	2.0	2.0	1.908
GER	P	550.5	16.1	67.1	0.8-2.8Hz	A0,C,D	2.0	2.0	2.023
NRS	P	530.5	19.1	78.1	1-3 Hz	A0,C,D	1.0	2.0	1.133

Tr. time	--	Travel time of phase
App. vel.	--	Apparent velocity from broadband F-K measurement
Azim.	--	Azimuth from broadband F-K measurement
Filter	--	Cutoffs of bandpass filter (3rd order Butterworth)
Config.	--	Array configuration used in beamforming. A0,B,C means A0Z, B-ring and C-ring
STA_len.	--	STA length in seconds
Tim. tol.	--	Time tolerance when searching for maximum STA
STA_calib.	--	Calibration factor used when converting STA values (in quantum units) to magnitude Magnitude = $\log_{10}(\text{STA}) + \text{STA\_calib.}$

Table 7.1.1. Parameters used in threshold monitoring experiment.

	Day-of-Year					Total
	274	275	276	277	278	
$m_b \geq 5.0$	0	2	0	0	1	3
$m_b \geq 4.5$	0	3	0	0	1	4
$m_b \geq 4.0$	0	8	0	1	1	10
$m_b \geq 3.75$	1	13	0	2	3	19

Table 7.1.2. Statistics of peaks in the network threshold traces.

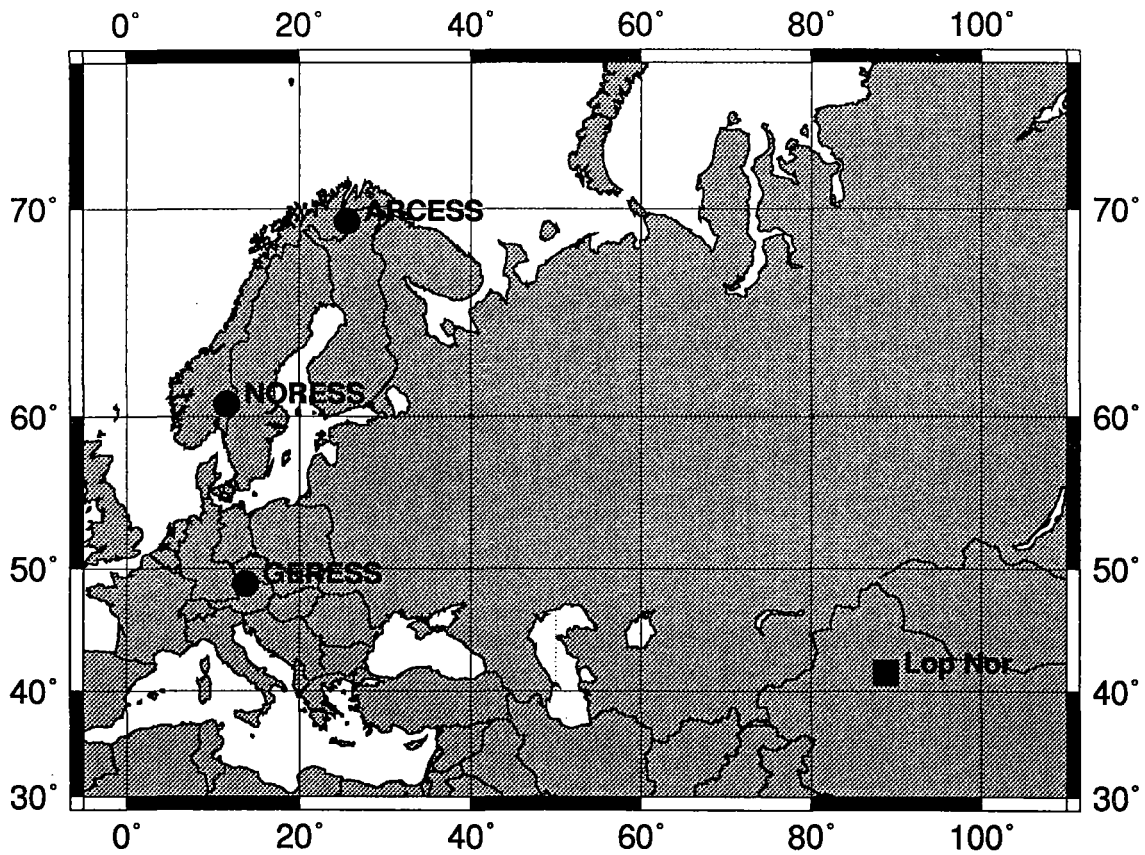


Fig. 7.1.1. Map showing the location of the Lop Nor test site and the three arrays used in the monitoring experiment.

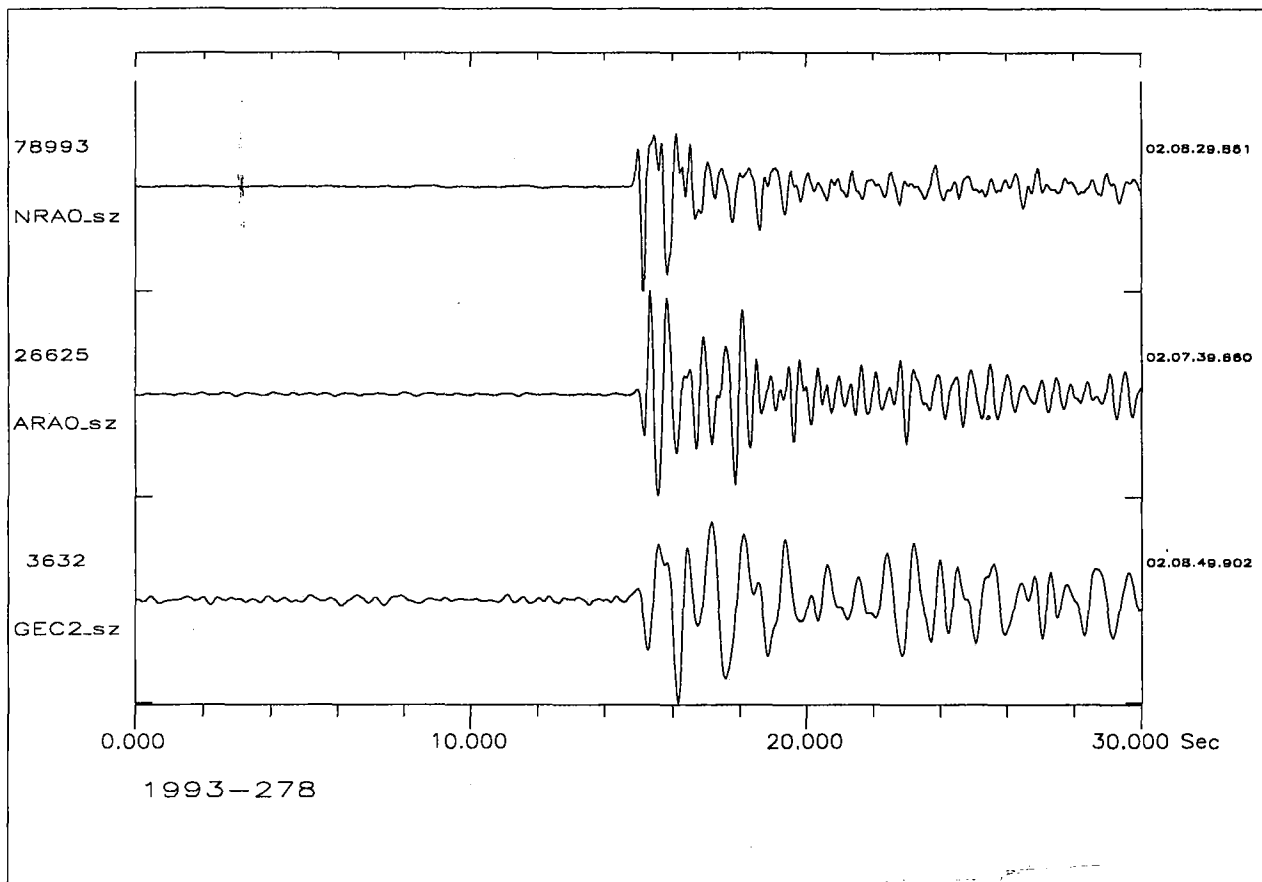
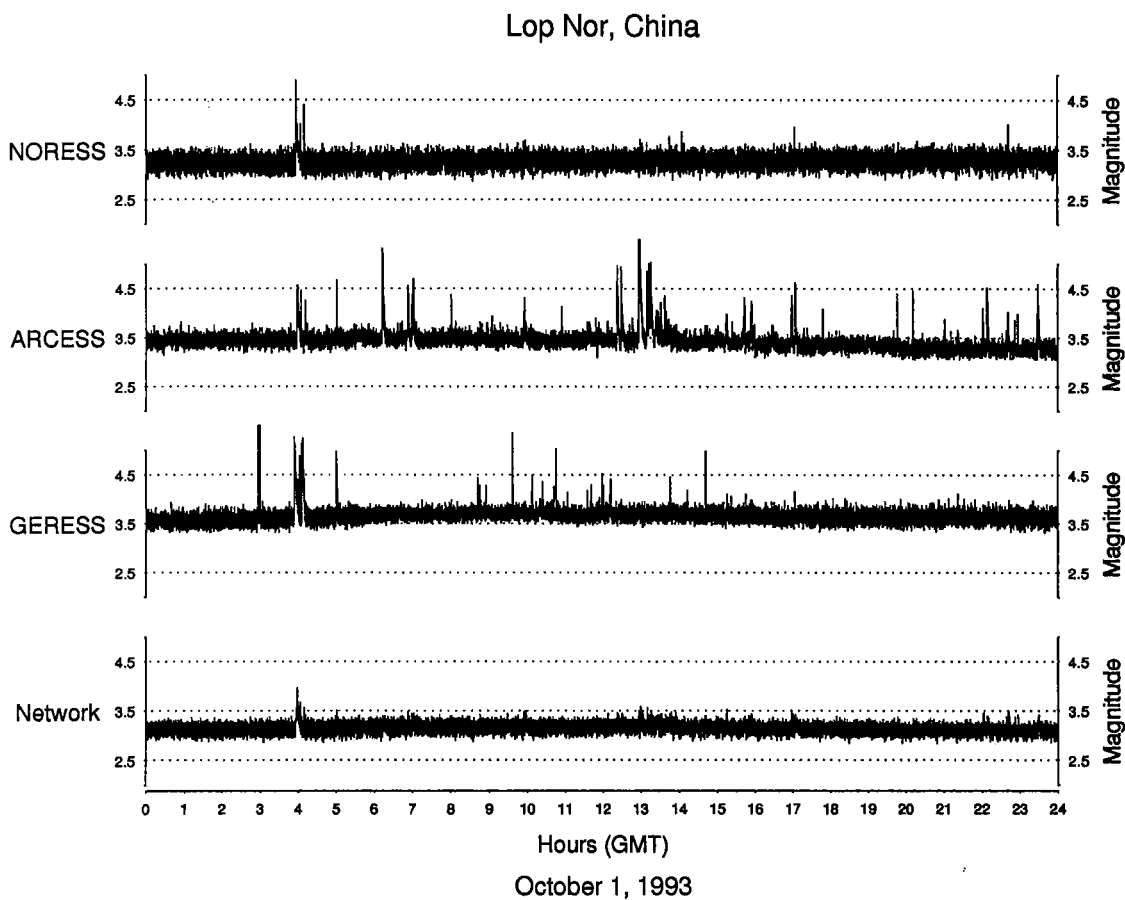
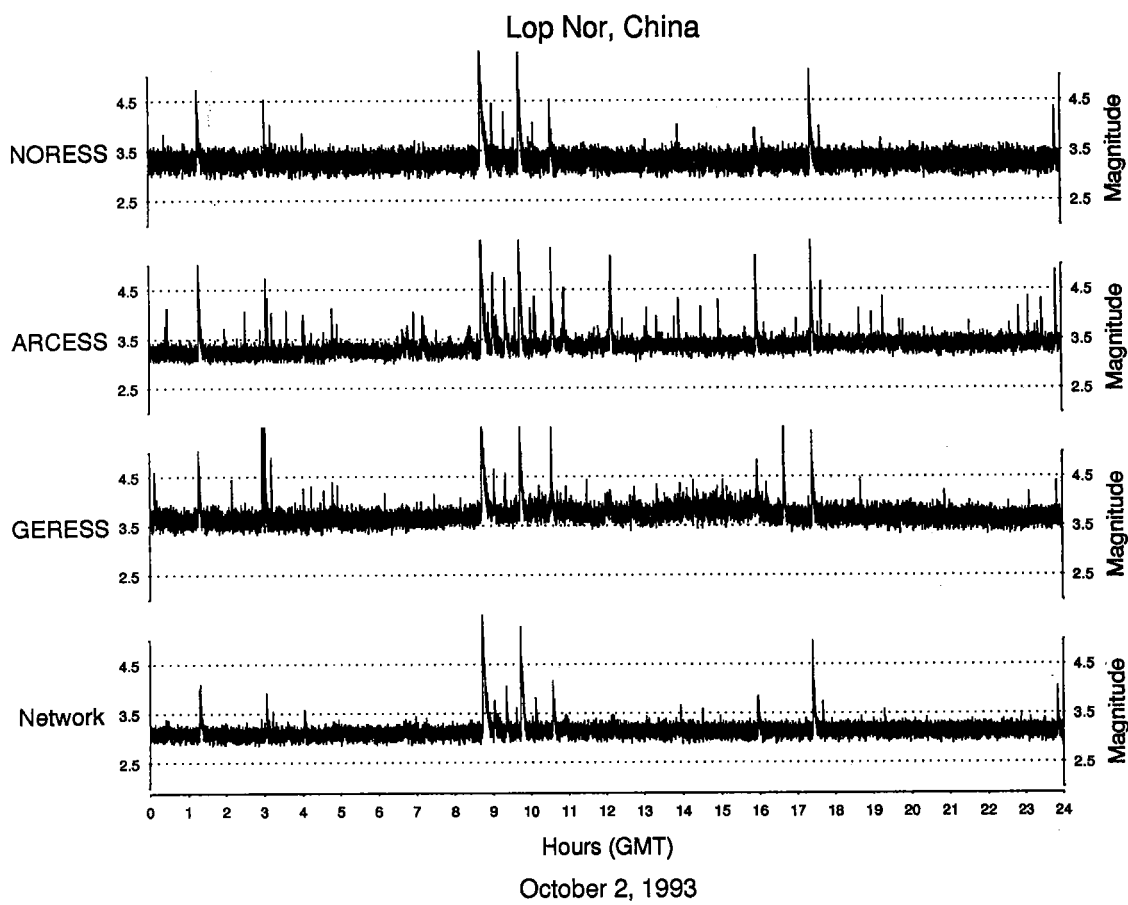


Fig. 7.1.2. NORESS, ARCESS and GERESS recordings of the Lop Nor explosion of 5 Oct 1993 ( $m_b \approx 5.9$ ).





**Fig. 7.1.3.** Threshold monitoring of the Novaya Zemlya test site for day 274 (1 October 1993). The top three traces represent thresholds (upper 90 per cent magnitude limits) obtained from each of the three arrays (ARCESS, NORESS, GERESS), whereas the bottom trace shows the combined network thresholds.



**Fig. 7.1.4.** Same as Fig. 7.1.3, but for day 275 (2 October 1993). The large number of threshold peaks are caused by an earthquake sequence in Sinkiang, China.

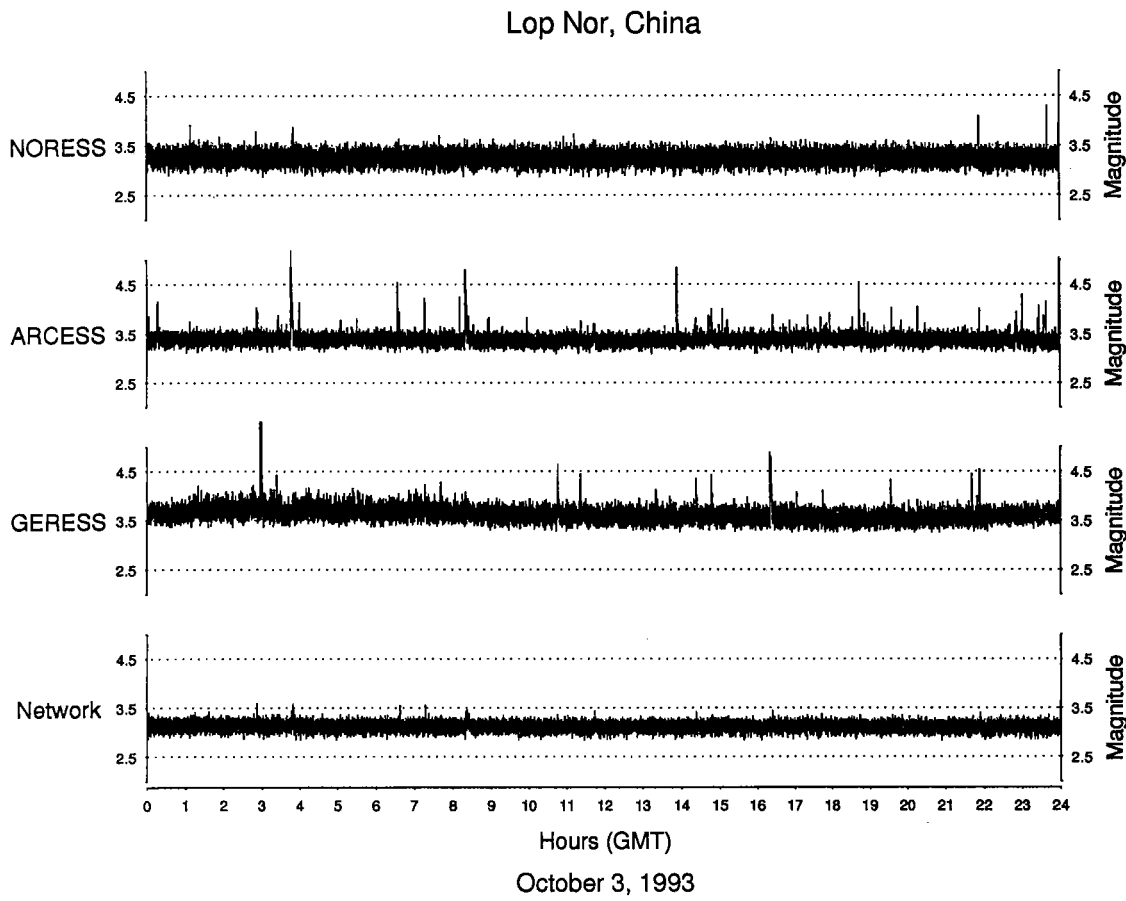
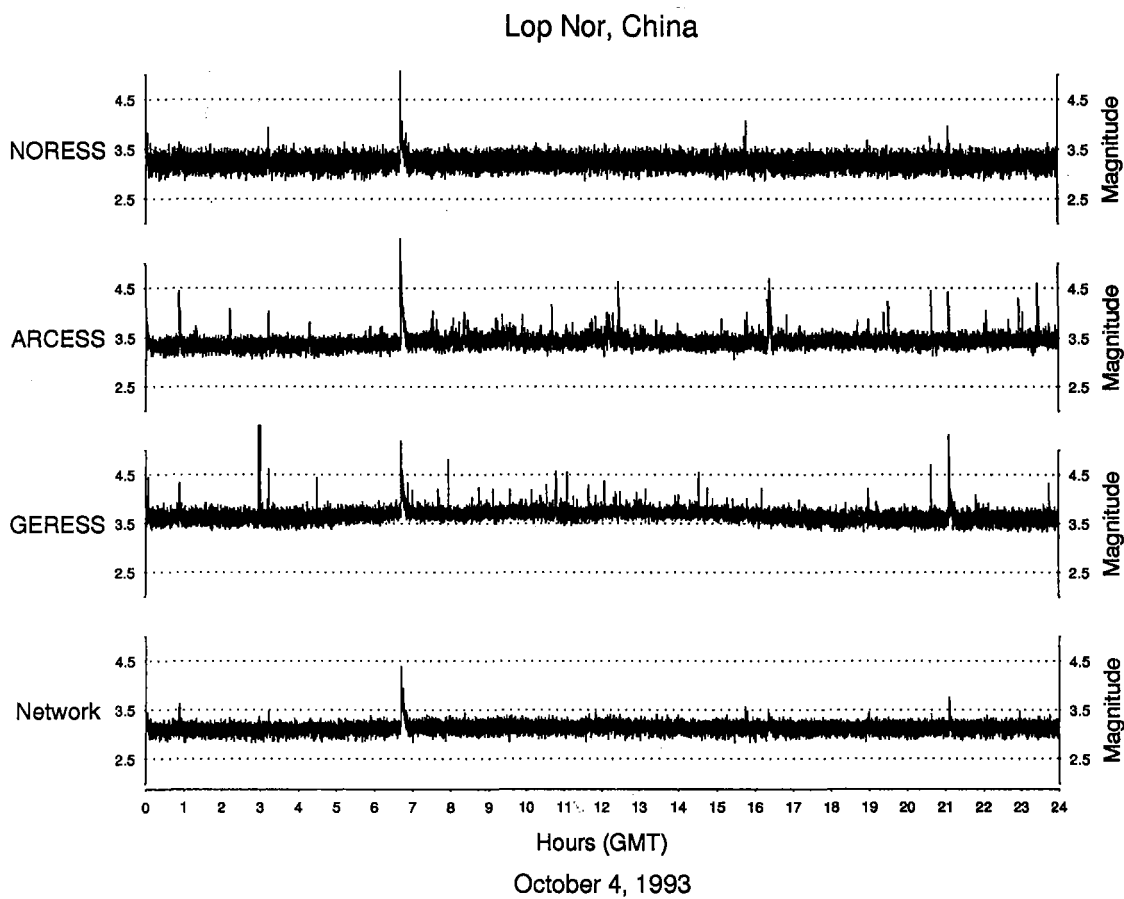
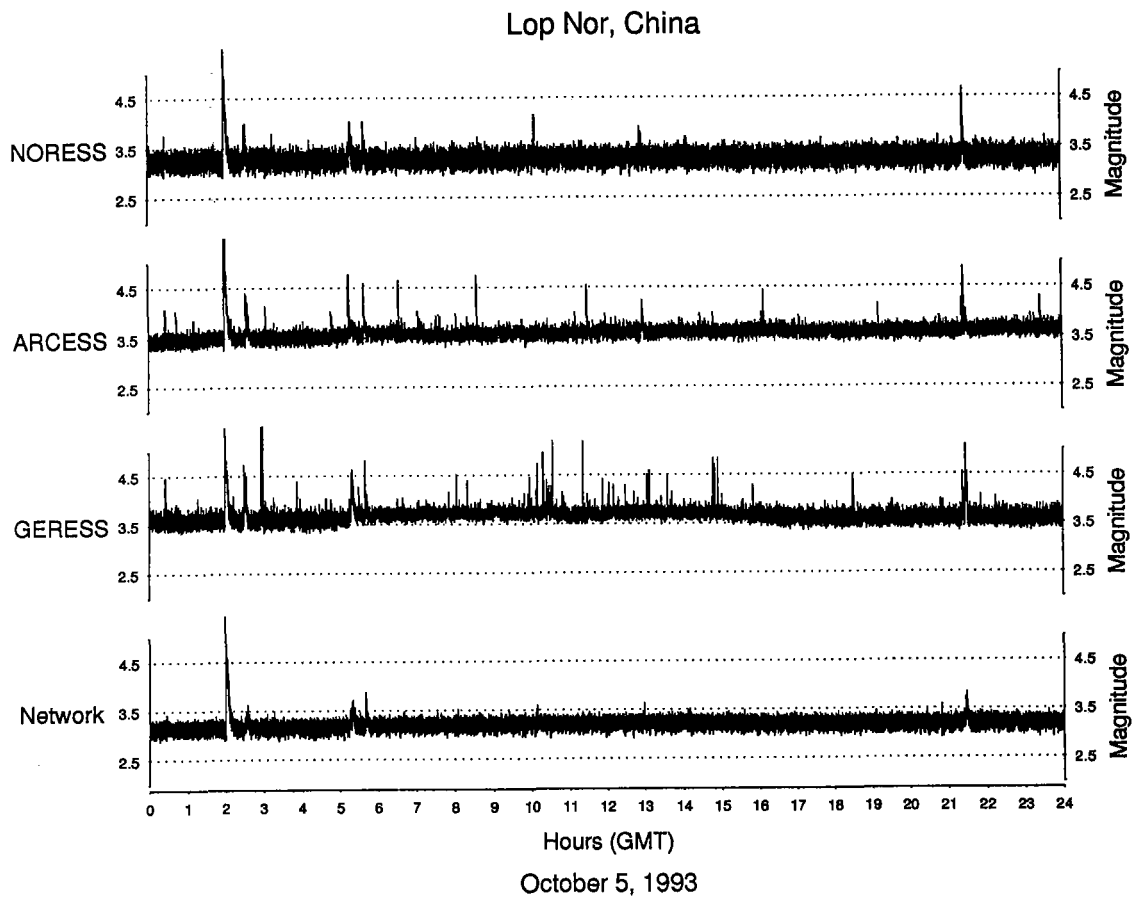


Fig. 7.1.5. Same as Fig. 7.1.3, but for day 276 (3 October 1993).



**Fig. 7.1.6.** Same as Fig. 7.1.3, but for day 277 (4 October 1993).



**Fig. 7.1.7.** Same as for Fig. 7.1.3, but for day 278 (5 October 1993). The threshold peak at 0200 hrs is due to the Lop Nor nuclear test.

### Threshold magnitudes - Lop Nor

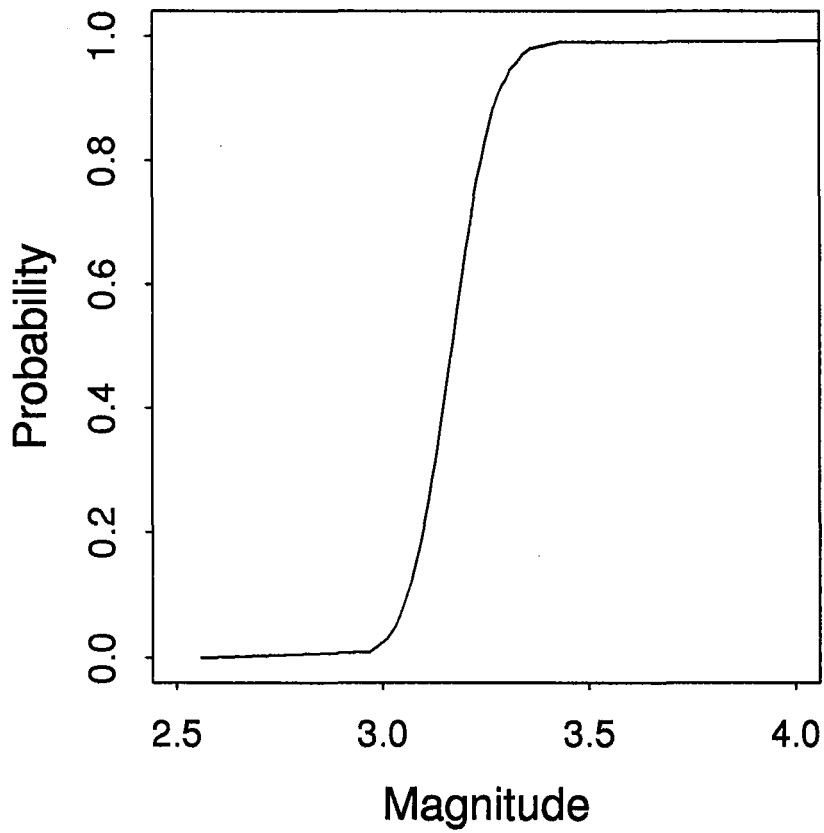


**Fig. 7.1.8.** Cumulative statistics of the network threshold magnitudes for the five-day period, 1-5 October 1993.